Retrievals of Atmospheric Temperature and Water Vapor in the Arctic

J.C. Liljegren and M.P. Cadeddu
Argonne National Laboratory
Argonne, Illinois

Abstract

We show that by incorporating brightness temperature measurements at off-zenith angles, the accuracy of linear statistical retrievals of temperature and water vapor density profiles can be improved. This improvement is limited to clear sky cases where measurements at all angles represent the same atmospheric conditions. We present contribution functions to show how the off-zenith measurements affect the retrieval performance. We show that the brightness temperatures calculated using the MonoRTM and modified Rosenkranz models are affected by the choice of spectroscopic parameters for microwave absorption by oxygen, and how these choices affect the retrievals.

We also show that by combining brightness temperature measurements near the 22.235-GHz water vapor line with measurements near the 183.31-GHz line into a physical retrieval, the accuracy of the retrieved water vapor density profile for very low water vapor conditions can be significantly improved.

Background

The Atmospheric Radiation Measurement (ARM) Program has operated a twelve-channel microwave radiometer profiler (MWRP) (Liljegren 2002) since February 2004 at ARM Climate Research Facility (ACRF) North Slope of Alaska (NSA) field site near Barrow, Alaska. The MWRP has five channels in the 22- to 30-GHz range and seven channels in the 50- to 60-GHz range that are used to derive vertical profiles of water vapor density and temperature, as well as the integrated precipitable water vapor and cloud liquid water path, at 5-minute intervals. These profiles are a valuable supplement to the collocated radiosondes launched Monday-Friday, once per day, at 2300 Universal Time Coordinates.

Contours of temperature and water vapor density obtained by using the MWRP are presented in Figure 1, revealing details of a frontal passage. In contrast to radiosondes, the MWRP provides substantially improved temporal resolution but coarser vertical resolution that declines in proportion to the height above ground level. A consequence of declining resolution with height is that temperature inversions and sharp water vapor gradients, as illustrated in Figure 1, can be difficult for passive profilers to resolve accurately. In this paper, we investigate improving the vertical resolution of

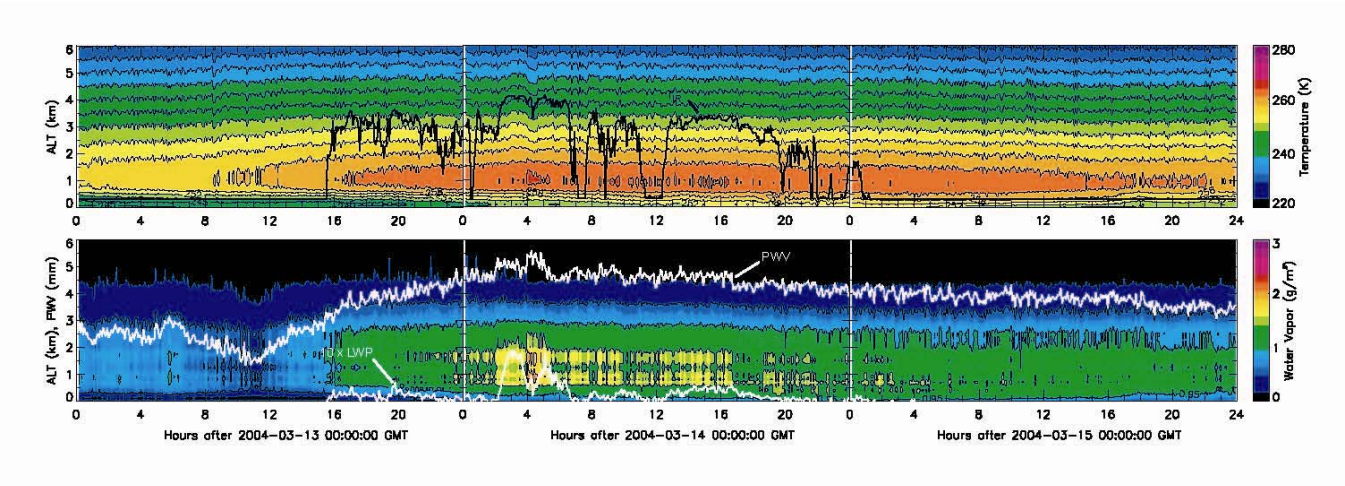

Figure 1. Time-height contours of temperature (top) and water vapor density (bottom) for 12-15 March 2004 at the ACRF NSA site at Barrow, Alaska. The black line in the top panel indicates the temperature reported by the infrared thermometer. The white line in the bottom panel indicates the precipitable water vapor.

temperature and water vapor density retrievals by adding off-zenith measurements. We also investigate the benefits of adding measurements near 183 GHz for improving the water vapor density profile retrieval.

Multi-Angle Retrievals

In addition to zenith, brightness temperatures are measured at elevation angles of 23.6°, 19.5°, and 16.6° symmetrically about the zenith for all K-band (22.235, 23.035, 23.835, 26.235, and 30.0 GHz) and V-band (51.25, 52.28, 53.85, 54.94, 56.66, 57.29, 58.80 GHz) channels. These angles correspond to air masses (= 1/sin(elev)) of 2.5, 3.0, and 3.5. Although these angles were selected to provide data for tipping-curve calibrations of the K-band channels (Liljegren 2000), they may also provide a means to improve the vertical resolution of the retrieved profiles (Gary 1988; Westwater et al. 2000) despite not being optimally selected for this purpose.

We developed a priori statistical retrievals for temperature and water vapor density profiles by using zenith measurements only and by using zenith plus off-zenith measurements as follows. Vaisala RS90 radiosondes launched during 2002-2005 were input to a microwave radiation transfer model (Schroeder and Westwater 1991) to compute brightness temperatures at the twelve measurement frequencies and four measurement angles. The model incorporates the Rosenkranz absorption model for oxygen and water vapor (Rosenkranz 1998, 2003) modified to use a narrower half-width for the 22-GHz water vapor line (Gamache and Fischer 2003; Liljegren et al. 2005) and the MT-CKD water vapor continuum formulation (Mlawer et al. 2003). K-band brightness temperatures were transformed to opacity by using mean radiation temperatures for each frequency and angle fitted to surface temperature, pressure, and relative humidity. Gaussian noise (mean = 0 K, standard deviation = 0.5 K) was added to the calculated

brightness temperatures to simulate an actual instrument. The a priori data were divided into four periods: spring (March-May), summer (June-August), fall (September-November), and winter (December-February). Retrieval coefficients for each season were determined by using the calculated K-band and V-band observables plus the surface pressure, temperature, and water vapor density.

To understand the effect of the off-zenith channels, the contribution functions (Rodgers 2000) were determined by perturbing the brightness temperature at each frequency and angle in succession by 1 K, then calculating the resulting change in the retrieved temperature or water vapor density profile. To more clearly illustrate the differences between the zenith-only and multi-angle retrievals, the contribution functions for the multi-angle retrievals were summed over all angles for each frequency. The contribution functions for temperature, presented in Figure 2, clearly show that the multi-angle retrieval contributions for the five upper V-band channels (53.85, 54.94, 56.66, 57.29, 58.80 GHz) are at lower levels. This is especially true at 53.85 GHz, which could degrade retrieval performance in the middle troposphere. The contribution of the 52.28-GHz channel to the zenith-only retrieval is negligible, whereas a small contribution is evident for the multi-angle retrieval; the 51.25-GHz channel contribution is very nearly the same for both retrievals. Contribution functions for the 51.25 and 52.28 GHz channels were non-negligible for the ACRF Southern Great Plains site (Liljegren 2002), which is approximately 320 m above sea level. This suggests these frequencies may not be optimal for the NSA site.

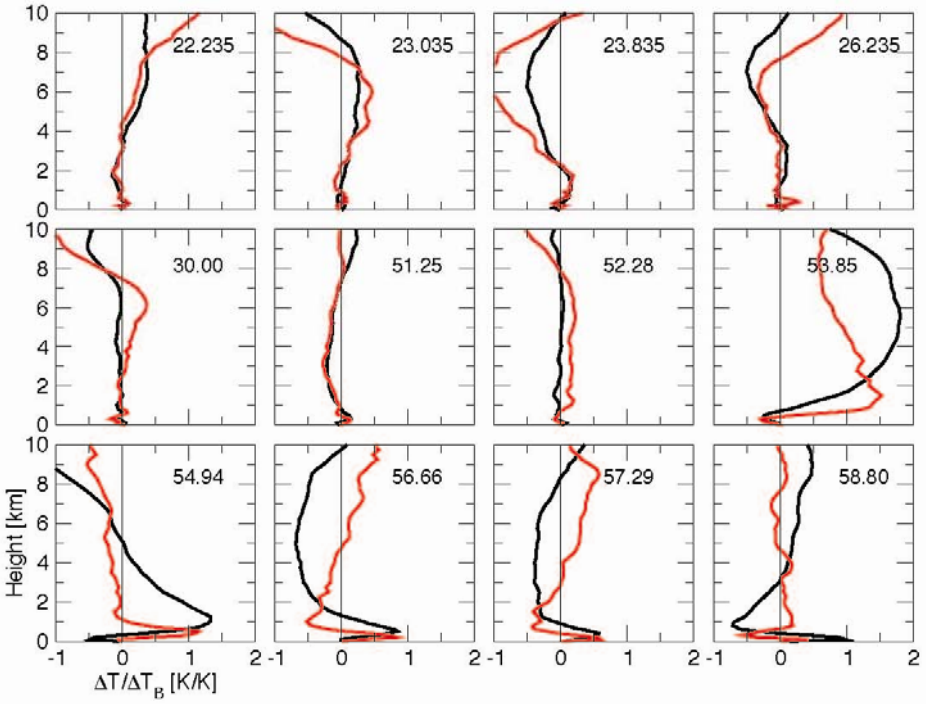

Figure 2. Contribution functions for the zenith-only (black) and multi-angle (red) temperature profile retrievals. All graphs have the same scale.

The contribution functions for water vapor density, presented in Figure 3, show little difference between zenith-only and multi-angle retrievals for the V-band channels, which is not surprising. The contributions of the 22.235-, 23.835-, and 26.235-GHz channels are qualitatively similar for both retrievals, although greater for the multi-angle retrieval. The lower- and middle-tropospheric contributions at 23.035 and 30.0 GHz are much greater for the multi-angle retrieval.

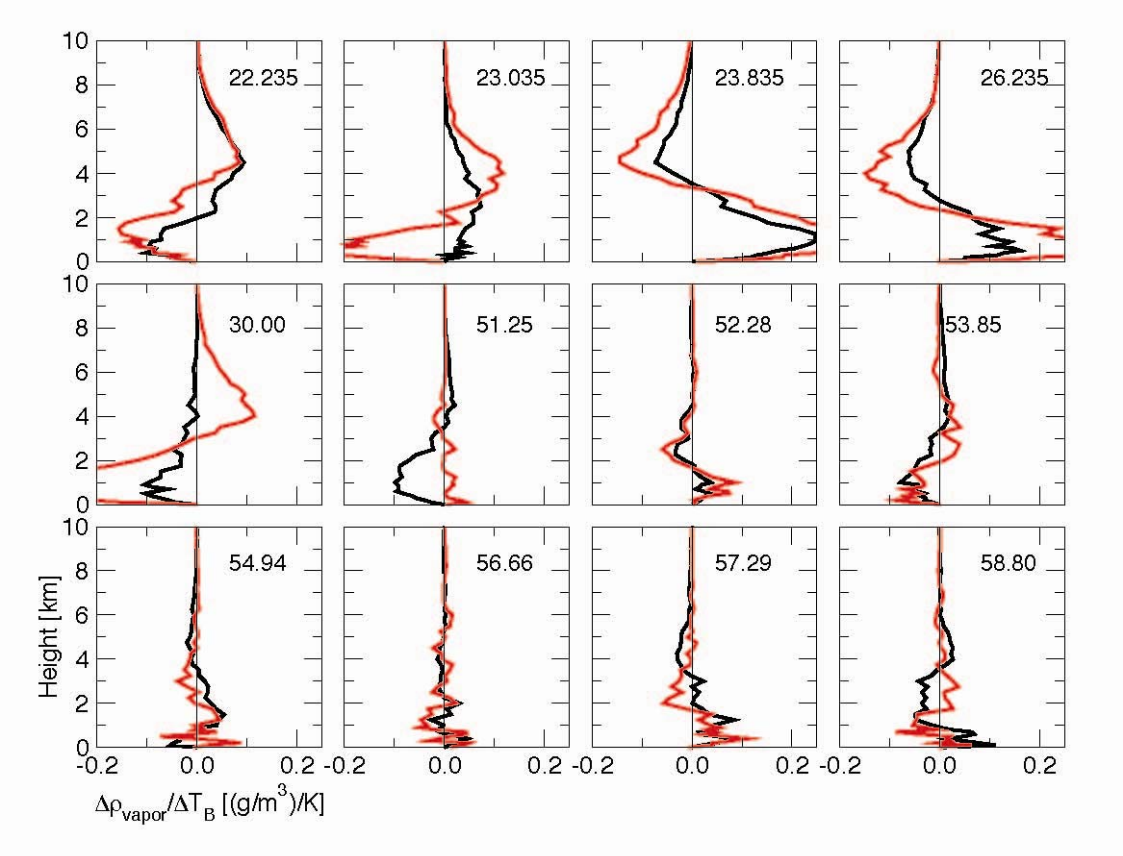

Figure 3. Contribution functions for the zenith-only (black) and multi-angle (red) water vapor density profile retrievals. All graphs have the same scale.

Practical Considerations

Several measurement issues must be addressed before applying the multi-angle retrievals. First, sky conditions must be horizontally uniform to ensure all angles are acquiring equivalent measurements. To enforce this condition, for each frequency, the square root of the sum of the squares of the brightness temperature differences between pairs of symmetric off-zenith angles had to be less than 4 K. This effectively limited measurements to clear sky conditions. Box plots of these root mean square (RMS) differences are presented in the upper panel of Figure 4. The trend in these results suggested a slight tilt

in the radiometer. This was confirmed by computing the RMS brightness temperature differences of model calculations at the nominal angles ± 0.5° as shown in the bottom panel in Figure 4. The calculations show the actual tilt is considerably less than 0.5°. To account for the tilt, the brightness temperatures of the symmetrical angle pairs were averaged before applying the multi-angle retrievals.

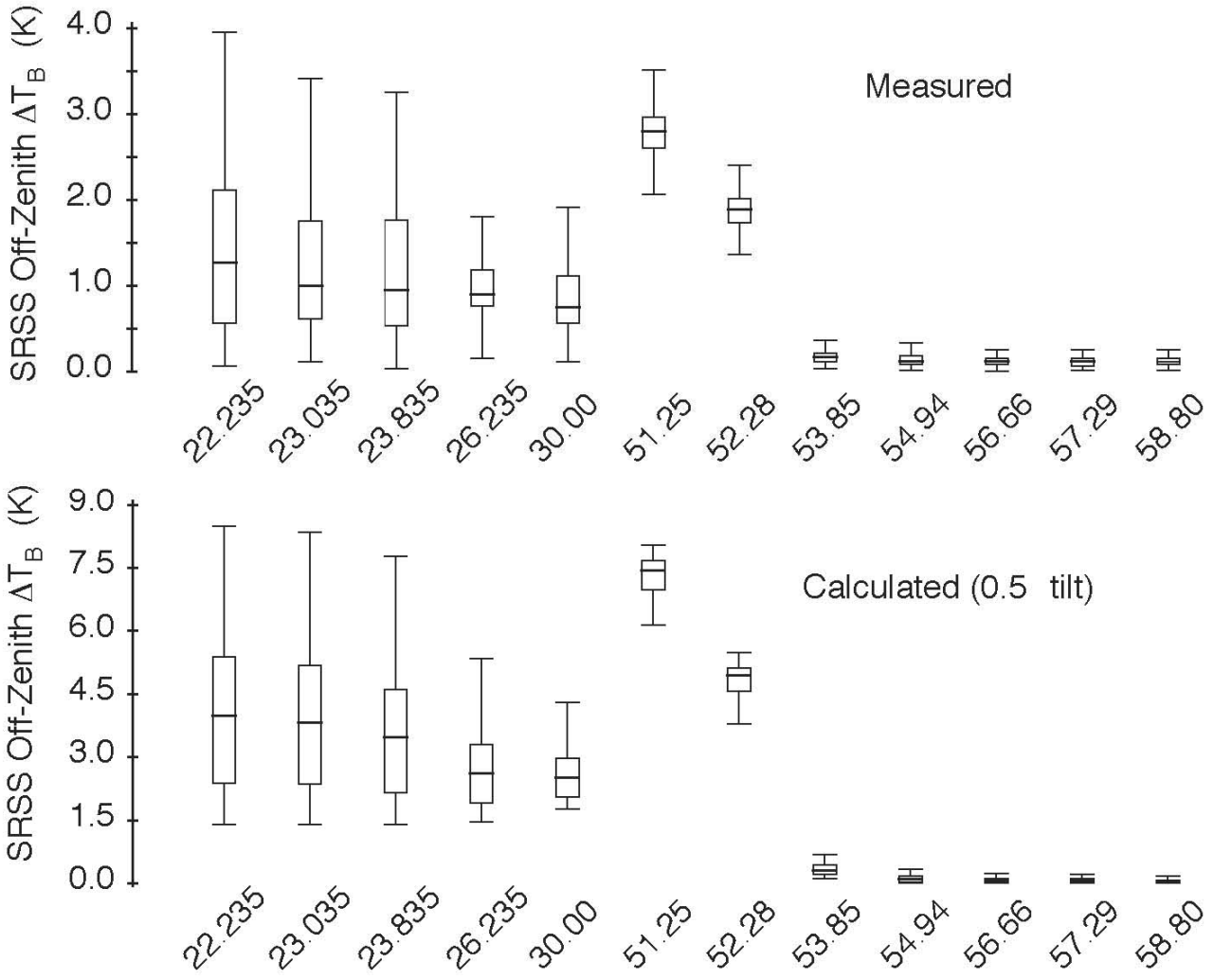

Figure 4. Box plots of the square root of the sum of the squares of the brightness temperature differences of the off-zenith angle pairs, [(23.6 – 156.4°)2 + (19.5° – 159.5°)2 + (16.6° – 163.4°)2]1/2 from measurements (top), and from model calculation for a 0.5° tilt (bottom).

A correction was applied to the off-zenith K-band brightness temperature to account for the finite beam width of the radiometer antenna (Liljegren 2000), which introduces a positive bias in the measured brightness temperatures that increases as the elevation angle decreases. The V-band measurements require no correction because the beam width at the V-band frequencies (~2°) is much less than for the K-band channels (~4.5-6°).

Spectroscopy and Modeling Issues

As the contribution functions illustrate, biases between the brightness temperatures measured by the radiometer and the model-calculated brightness temperatures used to derive the retrievals will result in biases in the retrieved temperature and water vapor density. Box plots of the differences between the measured and model-calculated V-band brightness temperature using three different combinations of model and spectroscopic parameters are presented in Figure 5. The comparisons are based on 196 radiosondes launched in close proximity to the MWRP between April 2004 and January 2006. Because radiosondes do not measure liquid water content, in addition to having to screen the cases on the basis of the RMS difference of the off-zenith angle measurements described earlier, the surface temperatures measured by the radiometer and the radiosonde had to agree within 3 K, and the 10-µm infrared sky temperature had to be less than 225 K to ensure liquid water-free conditions. The top panel (red) shows the results for the MonoRTM model (Boukabara et al. 1999) using the spectroscopic parameters for oxygen absorption from HITRAN. The middle panel (green) shows the results for MonoRTM using the more recent oxygen spectroscopy of Tretrakov (2005). The bottom panel (blue) shows the results for the modified Rosenkranz model, which also uses the Tretyakov oxygen spectroscopy. These results reveal the MonoRTM calculations using the HITRAN spectroscopy are biased low by 2-3 K at 51.25, 52.28, and 53.85 GHz. However, when the Tretyakov spectroscopy is used in MonoRTM, the calculations at 51.25 GHz are within 1 K of the measurements, whereas at 52.28 GHz the calculations are now biased high by 1 K. The comparisons at the remaining frequencies are not affected. The trend in the comparison with the modified Rosenkranz model is similar to MonoRTM using the Tretyakov spectroscopy: a slightly high bias at 51.25 and 53.85 GHz with a significant bias at 52.28 GHz. The spread of the differences for the modified Rosenkranz model is much less than for MonoRTM, which is independent of the spectroscopy and may reflect differences in the radiance calculations between the two models.

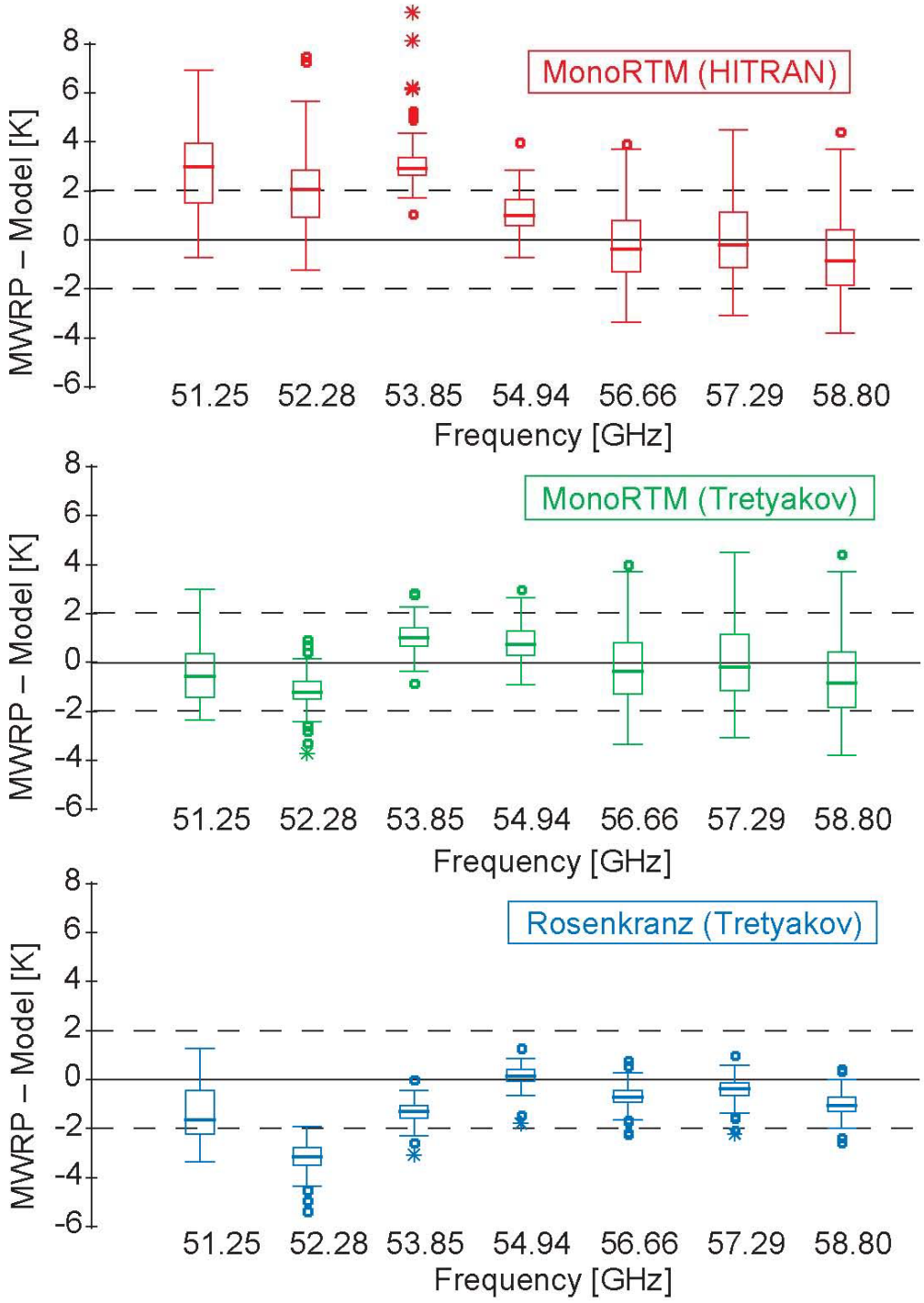

Figure 5. Box plots of measured minus calculated brightness temperatures for MonoRTM using spectroscopic parameters for oxygen absorption from HITRAN (top, red), for MonoRTM using oxygen parameters of Tretyakov (middle, green), and for modified Rosenkranz (bottom, blue) also using Tretyakov oxygen parameters.

Retrieval Results

The retrievals were applied to brightness temperatures measured with the MWRP and compared with the same 196 liquid-water free radiosondes used in the model comparisons described earlier. The ensemble mean (bias) and standard deviation of the differences (retrieval minus radiosonde) are presented in Figure 6a for temperature and Figure 6d for water vapor density. Significant biases between the retrievals and radiosondes are evident. For temperature, the multi-angle retrieval exhibits a greater bias than the zenith-only retrieval, whereas for water vapor density, the zenith-only retrieval has the larger bias. Although the bias at 52.28 GHz is the largest V-band bias, its effect on the temperature retrievals is small (negligible for the zenith-only retrieval). As the contribution functions show, the bias at 53.85 GHz is the most serious. Figure 6b shows the dramatic reduction in the temperature retrieval bias, and Figure 6e shows some improvement in the water vapor density bias resulting from subtracting the biases at 51.25, 52.28, and 53.85 GHz. Figure 6c and Figure 6f show that the standard deviations for the multi-angle and zenith-only retrievals are nearly identical above 1 km, but a slight improvement is evident below 1 km for the multi-angle retrievals.

Figure 7 presents a comparison of zenith-only and multi-angle retrievals compared with a radiosonde for 25 April 2005. The measured biases at 51.25, 52.28, and 53.85 GHz were subtracted before applying the retrievals. In this case, the multi-angle temperature retrieval resolves the elevated temperature inversion better than the zenith-only retrieval and agrees closely with the radiosonde. The multi-angle water vapor density retrieval is slightly improved relative to the zenith-only retrieval, but cannot resolve the sharp gradients evident in the radiosonde profile.

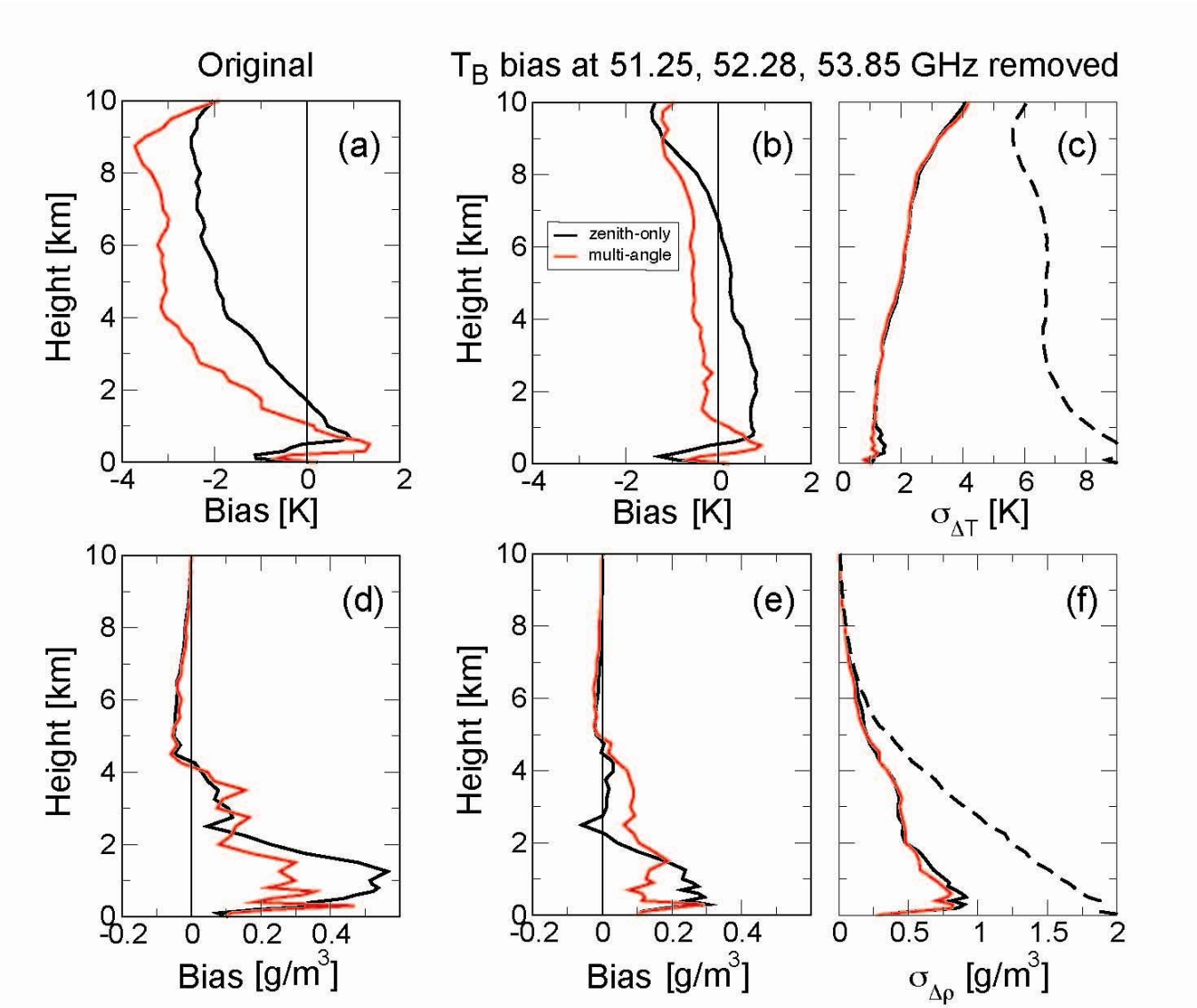

Figure 6. Mean of the retrieval-radiosonde differences (bias) in the temperature (a) and water vapor (d) profiles for the zenith-only retrievals (solid black line) and the multi-angle retrievals (red line); (b) and (e) same as (a) and (d) except the brightness temperature biases at 51.25, 52.28, and 53.85 GHz listed in Table 1 have been subtracted before applying the retrievals. The standard deviation of the retrieval-radiosonde differences is shown in (c) for temperature and in (f) for water vapor density; the standard deviation of the ensemble of radiosonde soundings around the mean of the ensemble is provided for reference (dashed black line).

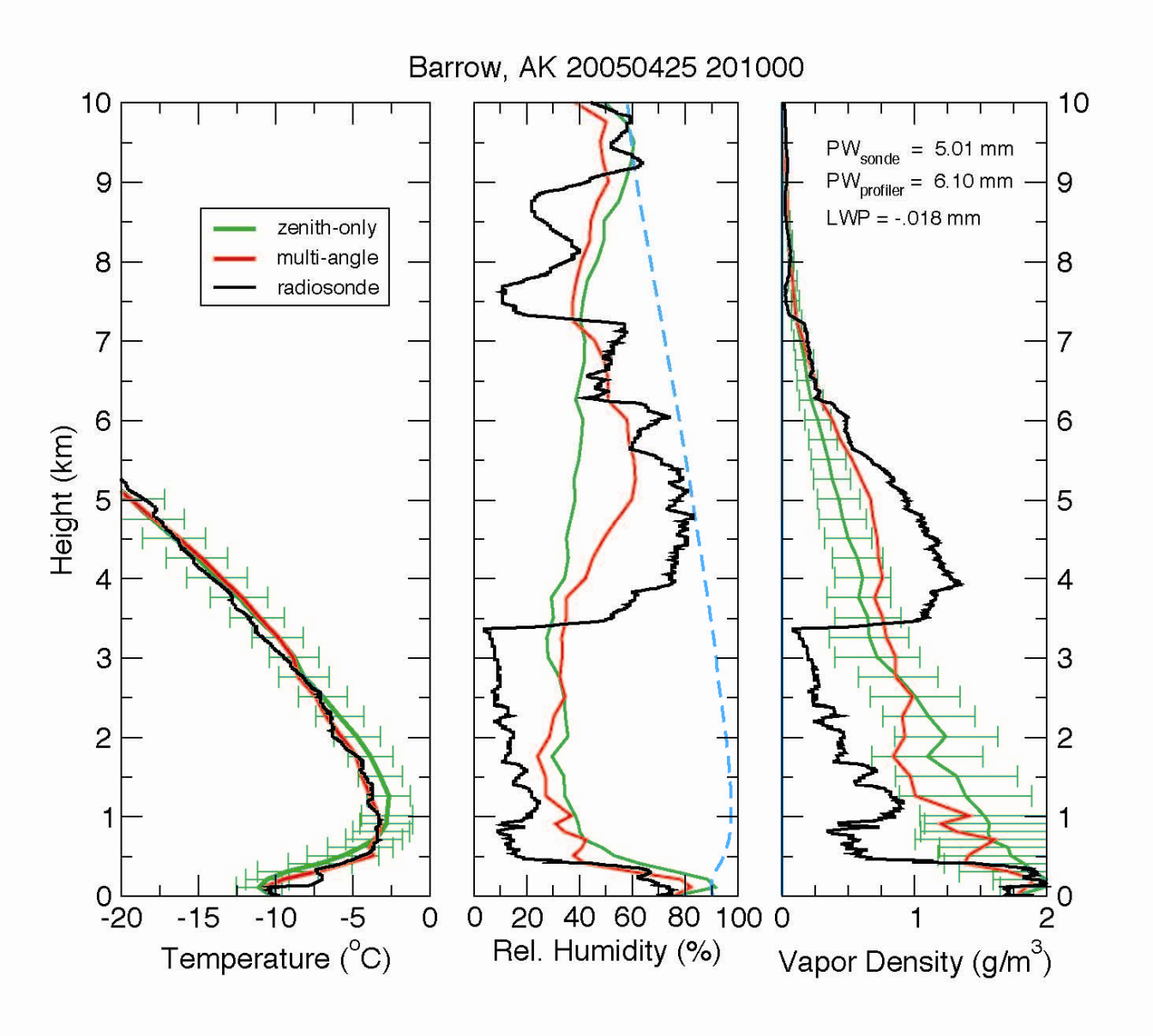

Figure 7. Profiles of temperature (left panel) and water vapor density (right panel) derived by using the zenith-only (red) and multi-angle (green) retrievals compared with radiosonde. The relative humidity (center panel) is calculated by using the retrieved temperature and water vapor density. The ratio of saturation vapor pressure over ice to saturation vapor pressure over liquid water (times 100) is represented by the dashed blue line in the center panel.

Combined MWRP and 183-GHz Retrievals

Iterative physical retrievals based on the MonoRTM model were developed to derive the water vapor density profiles from K-band measurements of the MWRP and brightness temperatures measured at 183.31 ±1, ±3, ±7, and ±14 GHz with the G-band water vapor radiometer (GVR) (Cadeddu et al.

2006a,b). Temperature profiles were derived by using the V-band MWRP channels alone. RMS brightness temperature errors of 2 K were used to account for the observed measured-modeled brightness temperature biases. The results of two cases are presented in Figure 8. In the first case, 12 December 2005, the additional GVR measurements have no effect. Both physical retrievals produce nearly identical results. The statistical retrieval results may be fortuitous because the brightness temperature biases have not been subtracted here.

In the second case, 25 January 2006, incorporating the GVR measurements into the retrieval clearly improves the result. The reason for the difference in performance between the two cases is that in the first case, the precipitable water vapor (PWV) was more than 3 mm, whereas in the second case, the PWV was less than 2 mm. Above 2 mm PWV, the 183±1 GHz channel begins to saturate and contributes little to the profile retrieval.

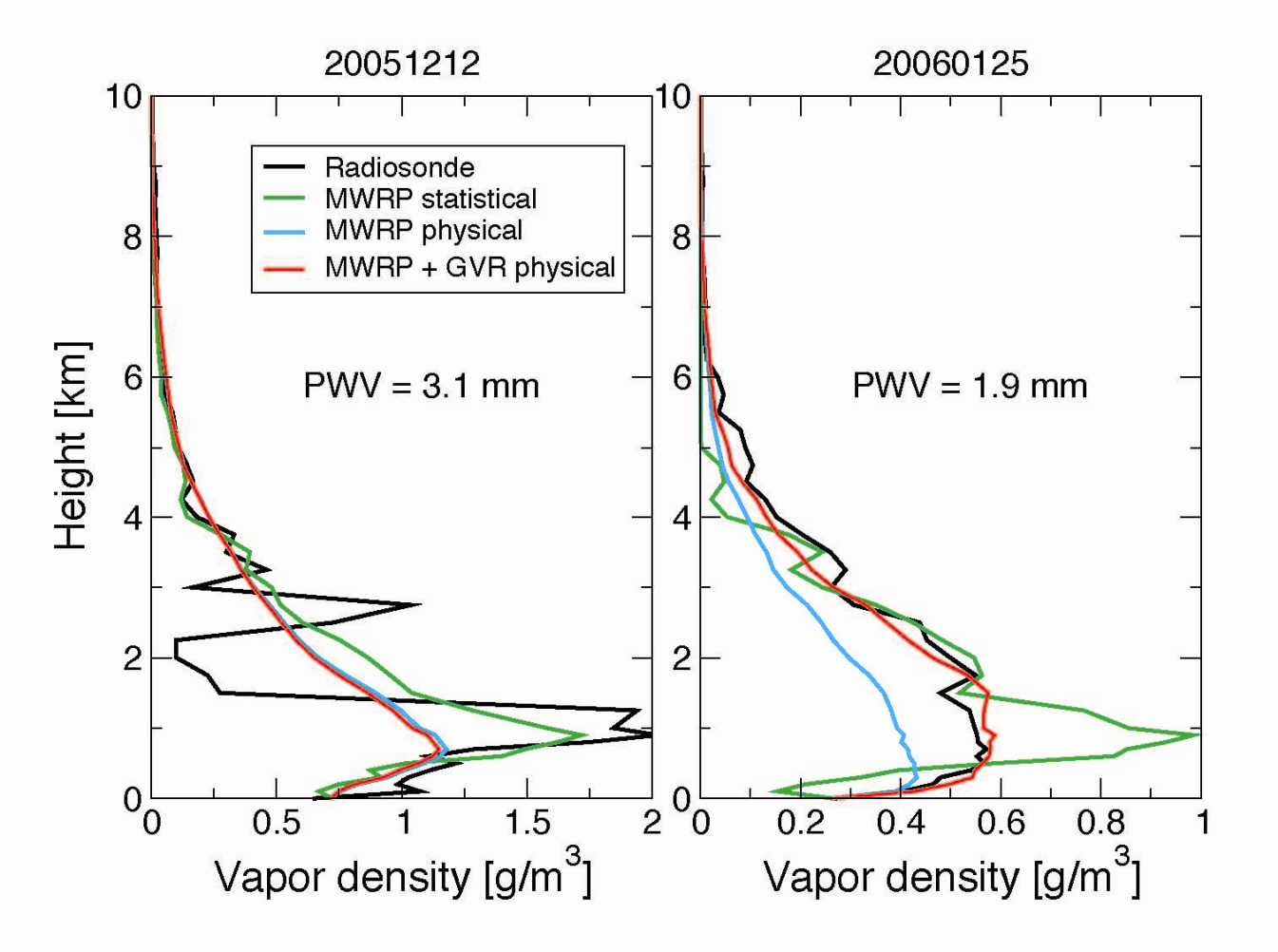

Figure 8. Profiles of water vapor density for 12 December 2005 (left) and 25 January 2006 (right) derived from the MWRP by using a statistical retrieval (red), a physical retrieval (green), with MWRP and GVR combined by using a physical retrieval (blue), and a radiosonde (black).

Conclusion

Statistical retrievals of temperature and water vapor density profiles have been developed for zenith-only and for multi-angle brightness temperature measurements in the 22- to 30-GHz and 50- to 60-GHz ranges. These have been applied to microwave radiometer measurements from Barrow, Alaska, for 2004-2006. Biases in the measured-modeled brightness temperatures at 51.25, 52.28, and 53.85 GHz, which may be due to spectroscopic issues with the oxygen absorption model, produce biases in both zenith-only and multi-angle temperature retrievals, as predicted by the contribution functions. A small (much less than 0.5°) tilt in the radiometer can significantly bias the brightness temperatures at low elevation angles, but averaging the brightness temperatures from symmetric angles on opposite sides of the zenith alleviates the problem.

For horizontally homogenous, clear sky conditions such that measurements at all angles represent equivalent conditions, the multi-angle retrievals offer better performance in the lowest 1-2 km, though at the cost of increased complexity. Using additional angles may further improve performance.

Utilizing the GVR measurements at 183.31±1, ±3, ±7, and ±14 GHz in addition to the five K-band channels of the MWRP can significantly improve the water vapor density profile retrievals for very low PWV conditions such that the ±1 and ±3 GHz channels retain sensitivity.

Acknowledgment

This work was supported by the Climate Change Research Division, U.S. Department of Energy, Office of Science, Office of Biological and Environmental Research, under contract W-31-109-Eng-38, as part of the Atmospheric Radiation Measurement Program. Argonne National Laboratory is managed by The University of Chicago for the U. S. Department of Energy.

Contact

James C. Liljegren
Argonne National Laboratory
9700 South Cass Avenue
Argonne, Illinois 60439
phone: 1-630-252-9540
email: jcliljegren@anl.gov

References

Boukabara, SA, SA Clough, and RN Hoffman. 1999. "MonoRTM: A monochromatic radiative transfer model for microwave and laser calculations." Twenty-second Annual Review of Atmospheric Transmission Models, Massachusetts.

Cadeddu, MP, K Kady-Pereira, SA Clough, and JC Liljegren. 2006a. "Improving the modeling of oxygen-band absorption: A model-measurement comparison." Preprints of the Ninth Specialists Meeting on Microwave Radiometry and Remote Sensing Applications, San Juan, Puerto Rico, 28 February-3 March.

Cadeddu, MP, JC Liljegren, and A Pazmany. 2006b. "Measurements and retrievals from a new 183-GHz water vapor radiometer in the Arctic." Preprints of the Ninth Specialists Meeting on Microwave Radiometry and Remote Sensing Applications, San Juan, Puerto Rico, 28 February-3 March.

Gamache, RR, and J Fischer. 2003. "Half-widths of H216O, H218O, H217O, HD16O, and D216O: I. Comparison between isotopomers." *Journal of Quantitative Spectroscopy and Radiative Transfer* 78:289-304, 2003.

Gary, BL. 1988. "Passive microwave temperature profiler." Report JPL-D-5484, Jet Propulsion Laboratory, California Institute of Technology, Pasadena, California.

Liljegren, JC. 2000. "Automatic self-calibration of ARM microwave radiometers." In *Microwave Radiometry and Remote Sensing of the Earth's Surface and Atmosphere*, P Pampaloni, S Paloscia, Eds., Zeist, The Netherlands: VSP Press, pp. 433-443.

Liljegren, JC. 2002. Evaluation of a new multi-frequency microwave radiometer for measuring the vertical distribution of temperature, water vapor, and cloud liquid water." Report ANL/DIS-05-04, Argonne National Laboratory, Argonne, Illinois.

Liljegren, JC, S-A Boukabara, K Cady-Pereira, and SA Clough. 2005. "The effect of the half-width of the 22-GHz water vapor line on retrievals of temperature and water vapor profiles with a 12-channel microwave radiometer." *IEEE Transactions of the Geosciences Remote Sensing* 43:1102-1108.

Mlawer, EJ, SA Clough, and DC Tobin. 2003. "The MT_CKD water vapor continuum: A revised perspective including collision induced effects." Presented at the Atmospheric Science from Space Using Fourier Transform Spectrometry (ASSFTS) Workshop, Bad Wildbad (Black Forest), Germany, 8-10 October.

Rodgers, CD. 2000. Inverse Methods for Atmospheric Sounding, Singapore: University Scientific.
.
Rosenkranz, P. 1998. "Water vapor continuum absorption: A comparison of measurements and models." *Radio Science* 33:919-928.

Rosenkranz, P. 2003. Private communication, August.

Schroeder, JA, and ER Westwater. 1991. Users guide to WPL microwave radiative transfer software. Report ERL-WPL-213, NOAA Environmental Research Laboratory, Boulder, Colorado.

Westwater, ER, Y Han, and F Solheim. 2000. "Resolution and accuracy of a multi-frequency scanning radiometer for temperature profiling." In *Microwave Radiometry and Remote Sensing of the Earth's Surface and Atmosphere*, P Pampaloni, S Paloscia, Eds., Zeist, The Netherlands: VSP Press, pp. 129-135.